



# Quantitative assessment of renal damage in rhesus monkeys with diabetic nephropathy using contrast-enhanced ultrasound

Hong Wang<sup>1</sup>, Xingxing An<sup>2</sup>, Yanrong Lu<sup>2</sup>, Wenwu Ling<sup>1\*</sup>, Yulan Peng<sup>1\*</sup>

<sup>1</sup>Department of Ultrasound, West China Hospital of Sichuan University, Chengdu, China; <sup>2</sup>Key Laboratory of Transplant Engineering and Immunology, West China Hospital of Sichuan University, Chengdu, China

**Contributions:** (I) Conception and design: Y Peng, W Ling; (II) Administrative support: W Ling; (III) Provision of study materials or patients: X An; (IV) Collection and assembly of data: H Wang; (V) Data analysis and interpretation: H Wang, Y Lu; (VI) Manuscript writing: All authors; (VII) Final approval of manuscript: All authors.

\*These authors contributed equally to this work and share corresponding authorship.

**Correspondence to:** Wenwu Ling; Yulan Peng. Department of Ultrasound, West China Hospital of Sichuan University, Chengdu 610041, China. Email: lingwenwubing@163.com; yulanpeng520@126.com.

**Background:** Diabetic nephropathy (DN) is a common chronic microvascular complication of diabetes. Noninvasive diagnosis of DN is difficult. Contrast-enhanced ultrasound (CEUS), as a functional imaging method, provides noninvasive real-time images and quantitative assessment of renal microvascular perfusion. This study investigated the efficacy of CEUS in discriminating between DN and normal kidneys in rhesus monkeys.

**Methods:** A total of 12 male rhesus monkeys (DN model group, n=6; normal control group, n=6) were included in this study. The following parameters were evaluated: (I) blood biochemistry; (II) CEUS; and (III) ultrasound-guided renal biopsy.

**Results:** Pathological and biochemical results showed that all subjects in the lesion group had serious renal damage. There were significant differences in the CEUS parameters, including the area under the curve, the time from peak to one half, and peak intensity between the lesion group and the normal group. The time to peak was slightly delayed in the lesion group. There was no significant difference in the rise time between the two groups.

**Conclusions:** Although the precise CEUS parameters that may best predict renal damage still require systematic evaluation, the results of these animal studies suggest that CEUS may be used as a supplemental tool in diagnosing renal damage in rhesus monkeys with DN. We hope these findings can provide insights for the application of CEUS in DN.

**Keywords:** Contrast-enhanced ultrasound (CEUS); rhesus monkeys; diabetic nephropathy (DN); renal damage; microvascular.

Submitted Jan 27, 2022. Accepted for publication Mar 16, 2022.

doi: 10.21037/atm-22-946

**View this article at:** <https://dx.doi.org/10.21037/atm-22-946>

## Introduction

Diabetic kidney disease or diabetic nephropathy (DN) is a progressive disease characterized by gradual damage of renal function. DN, which is one of the most severe diabetic microvascular complications, is the main etiology of chronic kidney disease and end-stage renal disease (ESRD) throughout the world (1,2). Studies have shown

that approximately 30% of type 1 and type 2 diabetics may develop DN (3,4). With the rapidly escalating number of patients with diabetes, DN greatly increases health costs and cardiovascular deterioration.

Nonhuman primates are the best candidate animal models for discovering and studying the mechanisms underlying human DN due to their close evolutionary

relationship. While most previous studies (5–8) have focused on the mechanisms and treatment of DN in rhesus monkeys, there is a paucity of data on renal blood perfusion. Studies in humans (9,10) have shown that renal blood perfusion is correlated with renal function. The diagnosis of DN in humans is often based on abnormalities in blood biochemical tests, including elevation of serum urea and creatinine concentrations, as well as the decline of urine specific gravity (11). Unfortunately, these abnormalities are often detected when there is already considerable renal dysfunction. Renal biopsy is the most commonly used diagnostic method. However, due to the associated risk of complications, such as hemorrhage, hematuria, or subcapsular hematoma after puncture, repeated renal biopsies play a limited role in humans and animal experiments. Contrast-enhanced ultrasound (CEUS) is a significant advancement in imaging techniques that allows noninvasive quantification of microvascular perfusion in tissues with corresponding quantitative parameters. Some studies (12–14) showed that CEUS could be used to evaluate renal blood flow perfusion and could identify DN in diabetic patients with kidney damage. However, there are few studies on quantitative CEUS parameters for discriminating DN and evaluating renal function failure. A recent study has found that the CEUS parameters could reflect pathological characteristics, especially changes in glomerular lesions (15). However, the consensus or corresponding guideline on how to evaluate DN with CEUS parameters, need to be further studied. Our previous pilot studies (16,17) examined insulin-deficient diabetes in rhesus monkeys with the aim of documenting the development of DN. In this current investigation, CEUS was applied to the evaluation of the precious rhesus monkey DN model, and the feasibility of CEUS parameters for the quantitative assessment of functional kidney damage in a DN model using rhesus monkeys was evaluated. It is beneficial to evaluate the renal damage of DN in further animal experiments. In this study, the animals in the lesion group had been diabetic for about 3 years. We present the following article in accordance with the ARRIVE reporting checklist (available at <https://atm.amegroups.com/article/view/10.21037/atm-22-946/rc>).

## Methods

A total of 12 male rhesus monkeys were acquired from a government-accredited experimental animal breeding and research base (Chengdu Pingan, Sichuan, China). A

protocol was prepared before the study without registration. Experiments were performed under a project license (No. 2018225A) granted by Ethics Committee of West China Hospital of Sichuan University, in compliance with the Guide for the Care and Use of Laboratory Animals, 8th edition. All animals had free access to water supply and were fed standard monkey diets twice a day.

Animals were divided into two groups, a lesion group and a control group, with 6 monkeys in each group. The diabetic model was established via intravenous injection of streptozotocin (Sigma-Aldrich, St. Louis, MO, USA), as previously described (18). The criteria for successful establishment of diabetes were fasting blood glucose (FBG) values  $>11.1$  mmol/L for 2 consecutive days and a C-peptide (C-P) concentration  $<0.5$  nmol/L. Exogenous insulin (Wanbang Biopharma Co. Ltd, Xuzhou, China) as a supplement was required to maintain an FBG level  $<15$  mmol/L, allow growth in juveniles, and to keep adults at an acceptable weight, so as to avoid frequent episodes of ketoacidosis. A previous longitudinal study (19) showed that long-term ( $\sim 3$  years) diabetes can lead to kidney injury in rhesus monkeys. Six male rhesus monkeys (5–8 years old, weighing 8.2–13.0 kg, with a mean weight of  $11.2 \pm 1.9$  kg) with diabetes for about 3 years were selected as the lesion group for the present study. A further 6 normal rhesus monkeys, matched for gender, weight, and age (aged 4–7 years, weighing 5.1–12.7 kg, with a mean weight of  $10.2 \pm 2.9$  kg) were used as normal controls. All subsequent operations were performed after sedation via intramuscular injection of ketamine (5 mg/kg) and midazolam (0.2 mg/kg).

Detailed conditions of the subjects were recorded, including weight, eating status, and behavioral pattern. Physical examination and laboratory testing were performed every 1–2 months. Considering the risk associated with complications of renal biopsy, all subjects underwent blood biochemical examination, ultrasound, CEUS, and ultrasound-guided core needle biopsy in sequence. Blood biochemistry was completed prior to the ultrasound examination. The hair of the abdomen was shaved by electric clippers for ultrasound. The coupling gel was applied to the abdomen of each rhesus monkey. All scans were performed with subjects lying in a supine or side position. Ultrasounds were performed with a scanner (iU22, Philips Medical systems) equipped with QLAB software to analyze and display time-intensity curves (TICs). First, greyscale ultrasound examinations of bilateral kidneys were performed using a high-frequency linear probe (3–9 MHz) in multiple sections and in multiple directions. The echo

(renal cortex, renal medulla, and collecting system) and presence or absence of occupancy were noted. A maximum longitudinal image displaying the entire kidney was used to perform the CEUS after injection of the ultrasound contrast agent. In this image, the whole kidney was centered on the screen, and the process of CEUS was captured with simultaneous B-mode and pulse inversion harmonic mode imaging. During the entire image acquisition process, the transducer was manually held at the same position. The mechanical index was set at 0.06, and adjusted parameters such as depth, gain, and focus were optimized and held constant during the study. An image capture time of 1 minute after the intravenous injection of the contrast agent was set. The ultrasound contrast agent SonoVue suspension (BraccoSpA, Milan, Italy) was administered by bolus injection (0.05 mL/kg) through the cubital vein of the subject, followed by rapid delivery of a 1.0-mL bolus saline for flushing. The injection was performed with a unified standard manner by the same person with CEUS nursing experience. There was an interval of at least 20 minutes between the 2 kidney CEUS examinations in each monkey, and the residual bubbles were cleared off with a flash echo technique at a high mechanical index setting.

All images obtained from the CEUS were stored on magnetic optical disks offline and analyzed using a commercially available software tool (Qlab, Philips). Three regions of interest (ROIs) in the renal parenchyma of each kidney were manually drawn by an ultrasound doctor (with more than 5 years' experience in CEUS imaging analysis) who was blinded to the groups. For every ROI, the size and depth were similar. The software was used to automatically generate a TIC using a fitting technique and related quantitative parameter values, including rise time (RT, sec, contrast agent perfusion time in ROI, from 5% to 95% of an increasing curve), peak intensity (PI, dB, the peak intensity of the contrast agent signal), area under the curve (AUC, dBsec, the area under the TIC curve), time from peak to one half (TPH, sec, time needed after injection when the intensity decreases to half PI), and time to peak (TTP, sec, the time after injection when the ROI signal intensity reaches its maximum).

Ultrasound-guided bilateral renal biopsies were conducted in each rhesus monkey at the end of CEUS. The puncture point was the lower pole of the kidney. The renal biopsy samples were placed in formalin. Hematoxylin-eosin (HE) staining was performed and the slides were observed under light microscopy by researchers who were blinded to the groups. All samples were assessed according to the

pathological diagnostic criteria of DN (glomerular basement membrane thickening, diffuse mesangial expansion, and/or Kimmelstiel-Wilson nodules).

### *Statistical analysis*

All statistical analyses were performed with the SPSS 20.0 software package. When the results of measurement data followed normal distribution and homogeneity of variance, data were expressed as the mean  $\pm$  standard deviation (SD). Continuous variables were evaluated with the Student's *t*-test. If the results did not conform to normal distribution, the Wilcoxon rank sum test was used. A *P* value  $<0.05$  (two-sided test) was considered statistically significant.

## **Results**

### *Blood biochemical indicators*

As shown in *Table 1*, the levels of uric acid (UA), creatinine (CREA), high-density lipoprotein (HDL), low-density lipoprotein (LDL), triglyceride (TG), direct bilirubin (DBIL), alanine aminotransferase (ALT), and aspartate aminotransferase (AST) were all increased in the lesion group compared to the control group. In contrast, the levels of LDH in the lesion group decreased significantly compared to the control monkeys. These indicators showed that the animals in the lesion group had severe kidney and liver damage.

### *Contrast enhance ultrasound (CEUS)*

All subjects completed ultrasound examinations successfully. There was no evidence of focal or diffuse abnormalities in any of the subjects. Renal echo did not show obvious changes in B-mode ultrasound in either group of animals. There was no evidence of space-occupying lesions in the kidneys. In the CEUS, the renal hilus first enhanced visually after the injection of SonoVue and rapidly spread to the renal artery, intrarenal arteries, and the renal cortex in sequence. The medulla and intrarenal vein were then observed in sequence (*Figure 1*). A significant visual difference was detected between the acquisition time (wash-in) and release of the contrast agent time (wash-out). Quantitative analysis of the renal parenchyma was performed using specialized computer software (QLAB). The TICs were generated in selected regions of the bilateral renal parenchyma. The shapes of the TICs in

**Table 1** The biochemical parameters in the lesion group and the control group

Index	Control group	Lesion group
Number	6	6
Age (years)	4–7	5–8
Weight (kg)	10.2±2.9	11.2±1.9
WBC (10 <sup>9</sup> /L)	10.01±4.03	9.62±4.04
MCV (fL)	68.75±3.75	66.3±3.67
MCH (pg)	24.44±1.23	24.01±1.34
MCHC (g/L)	357.54±12.84	362±6.68
ALB (g/L)	45.23±7.41	43.66±9.71
ALT* (g/L)	48.67±20.43	77.36±29.56
AST* (g/L)	35.6±17.78	83.11±25.47
GGT (IU/L)	89.0±37.9	93.63±43.84
DBIL* (IU/L)	0.43±0.20	1.3±0.7
CREA* (mmol/L)	50.84±13.23	75.74±17.24
HDL* (IU/L)	1.12±0.23	1.7±0.58
LDH* (μmol/L)	427.32±159.54	266.86±87.49
LDL* (mmol/L)	1.12±0.31	1.79±0.45
TBIL (IU/L)	2.84±0.41	2.77±0.75
TG* (IU/L)	0.54±0.02	0.94±0.71
UA* (μmol/L)	0.46±0.48	6.04±1.03
BUN (μmol/L)	6.96±1.24	7.09±1.39

Values are presented as the mean ± standard error. \*, P<0.05. WBC, white blood cells; MCV, mean corpuscular volume; MCH, mean corpuscular hemoglobin; MCHC, mean corpuscular hemoglobin concentration; ALB, albumin; ALT, alanine aminotransferase; AST, aspartate aminotransferase; DBIL, direct bilirubin; CREA, creatinine; HDL, high-density lipoprotein; LDH, lactate dehydrogenase; LDL, low-density lipoprotein; TG, triglyceride; TBIL, total bilirubin; UA, uric acid; BUN, blood urea nitrogen.

all experimental animals were asymmetric and unimodal with obvious ascending, descending, and peak shapes. The profile of the TIC showed a fast ascending branch and a slow descending branch (Figure 2). The overall shape of the curve in the lesion group (Figure 2A) was wide, ascended slowly, and descended sharply compared with the normal control group (Figure 2B).

The perfusion parameters of the TIC in the two groups followed a normal distribution. Compared with the normal

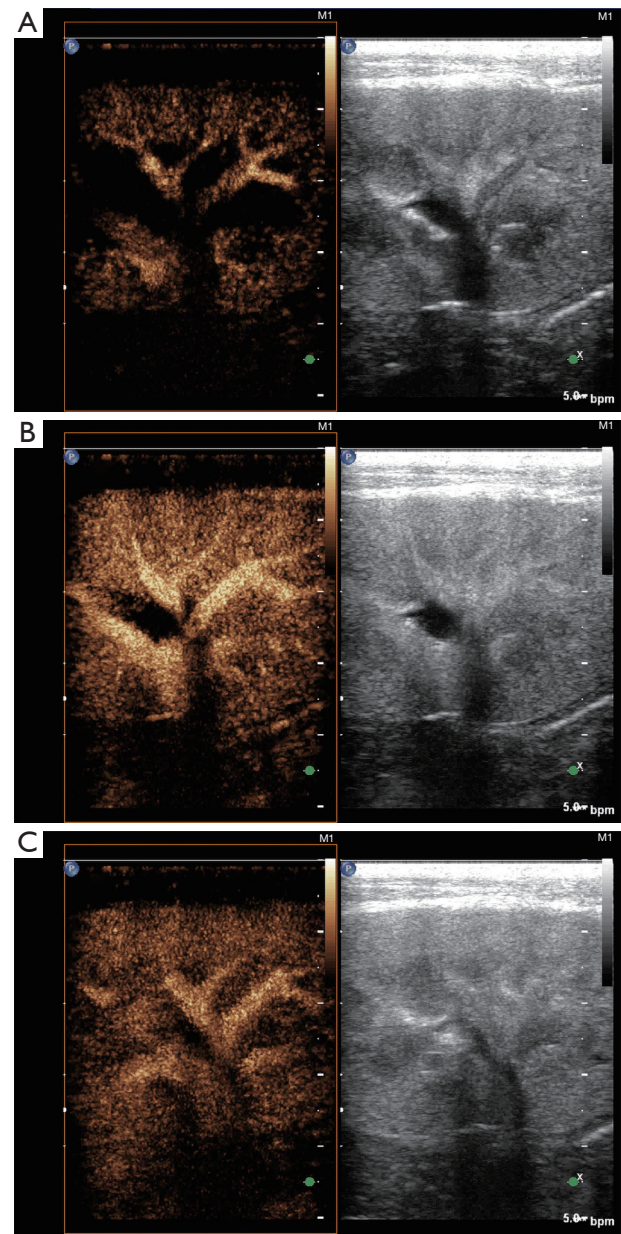


**Figure 1** A contrast-enhanced ultrasound performed on the kidney of a normal rhesus monkey. (A) The contrast agent reached the renal parenchyma 10 seconds after the bolus injection; (B) the intensity of the renal parenchyma reached its peak at 18 seconds after the bolus injection; (C) the contrast agent faded away 50 seconds after the bolus injection.

group, the lesion group showed significantly decreased PI, reduced AUC, the delayed TTP, and earlier TPH (P<0.05; Table 2). There was no significant difference in the RT

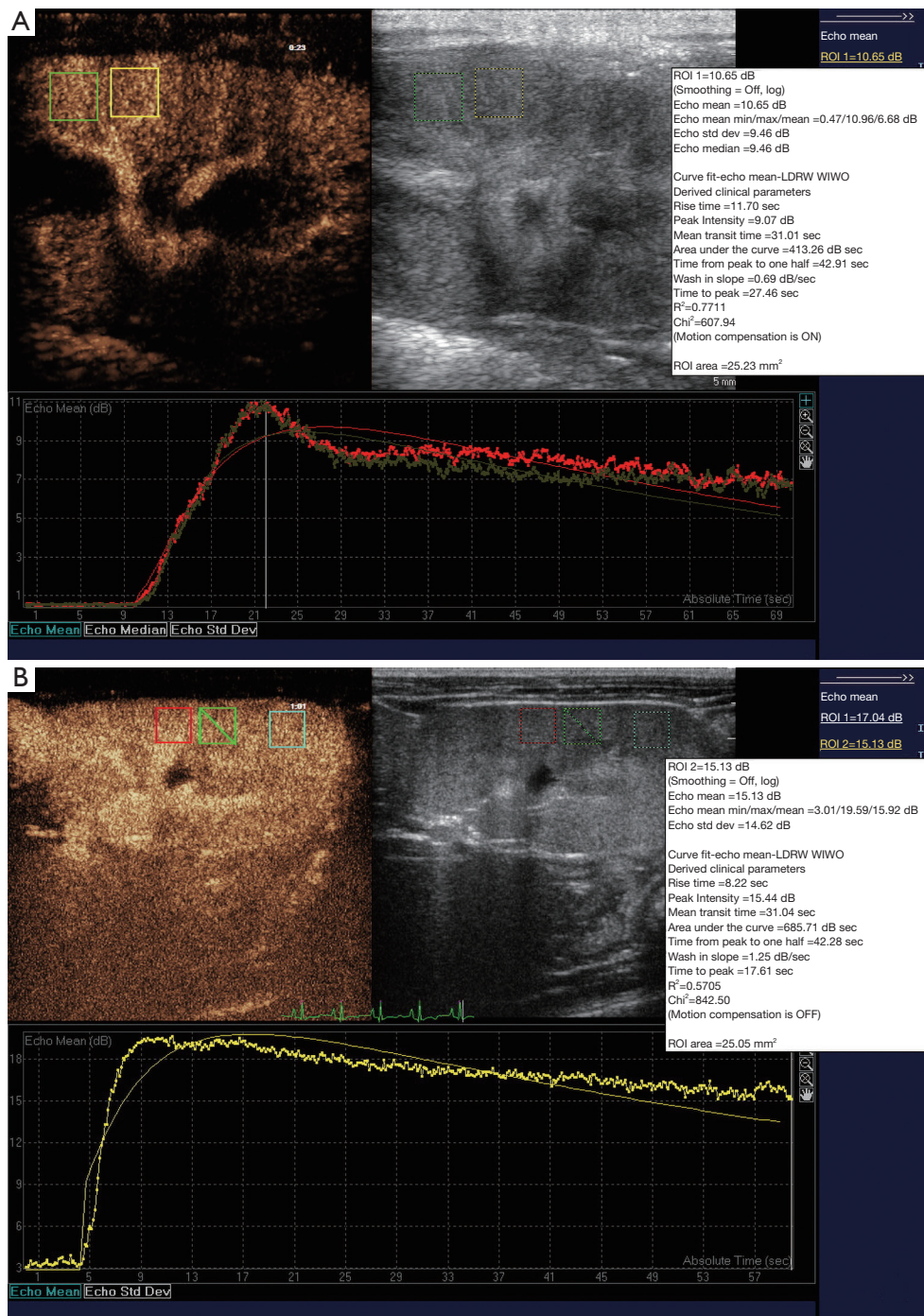


**Figure 2** The time-intensity curve of the renal parenchyma. (A) The overall shape of the curve was wide, ascended slowly, and descended sharply in the lesion group; (B) compared with the lesion group, the curve of the control group rose sharply, and then decreased slowly. These boxes of different colors represent the different regions of interest (ROIs) in the renal parenchyma of each kidney that were manually drawn by ultrasound doctor.

**Table 2** TIC parameters in the lesion group and the control group

Group	AUC* (dB sec)	TPH* (sec)	PI* (dB)	TTP* (sec)	RT (sec)
Control group	563.39±72.71	39.6±2.05	13.0±1.7	17.3±2.02	7.95±1.12
Lesion group	419.00±91.82	35.40±4.48	11.59±2.30	23.20±5.40	8.29±1.65

\*,  $P < 0.05$ . TIC, time intensity curve; AUC, area under the curve; TPH, time from peak to one half; PI, peak intensity; TTP, time to peak; RT, rise time.

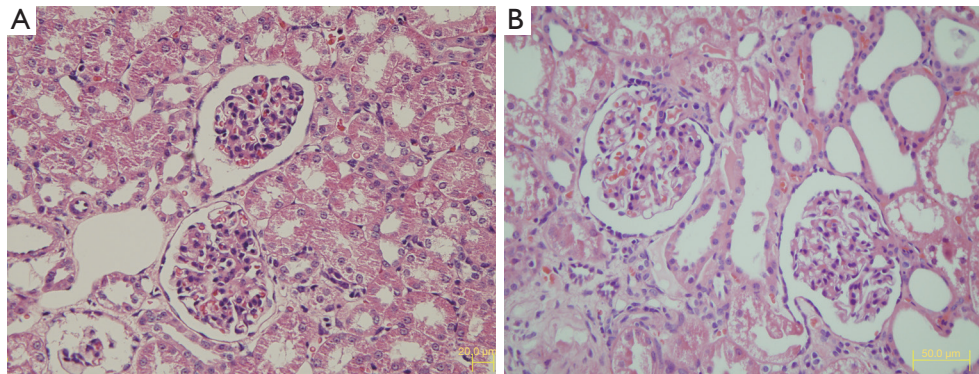


**Figure 3** Histology of the renal biopsies. (A) Photomicrograph of the renal tissue sections in the control group showing the normal histological structure of the glomerulus (hematoxylin and eosin staining); (B) photomicrograph of the renal tissue sections in the lesion group showing the swollen renal tubules, glomerular capillary basement membrane thickening, and mesangial matrix expansion (hematoxylin and eosin staining).

between the two groups.

### Renal histology

In accordance with the pathological criteria, all 6 rhesus monkeys in the lesion group were diagnosed with DN. Diffuse expansion of the mesangial matrix was observed in most diabetic monkeys (*Figure 3*). In addition, the peripheral glomerular basement membrane (PGBM) was thickened and mesangial cell proliferation was observed.

### Discussion

A kidney biopsy, the gold standard test for diagnostic, therapeutic regimen adjustment and prognostic information, is usually only performed when the renal pathology needs to be determined. At present, screening and diagnosis of DN is still based on the albuminuria assessment (20). The treatment of DN has two primary goals: preserving renal function to reduce the risk of ESRD; reducing the risk of cardiovascular events and mortality (21). For patients with typical DN, standard treatment still focuses on glycemic

and blood pressure control, with the aim of preventing DN progression and albuminuria regression (20).

Pathologically, DN is a secondary lesion to severe microvascular complications of diabetes (2). The process of disease progression is accompanied by glomerular basal membrane thickening, mesangial hyperplasia, and glomerular sclerosis. At present, the noninvasive diagnosis of DN in experiments using animals is mainly based on laboratory examination of blood and urine parameters. However, laboratory indicators cannot easily detect early diabetic renal damage and can be influenced by many external factors (such as proteinuria due to body stress, infection, hyperglycemia, hypertension, etc.). Therefore, the extent of renal damage cannot be objectively evaluated. Although renal needle biopsy is more sensitive and accurate, it is traumatic and risky to some extent. Therefore, it is necessary to explore sensitive, effective, and objective examination methods for the early and repeated quantitation of renal function. In a study involving healthy cats, CEUS has been used to detect differences in renal perfusion induced by angiotensin II (22). Renal perfusion changes have also been evaluated by using CEUS in renal ischemia-

reperfusion injury in dogs (23). These studies suggested that CEUS quantitative evaluation of renal perfusion is a valuable method for estimating renal perfusion changes in animal experiments.

Herein, a DN animal model was established to explore the changes in renal perfusion and blood biochemistry indicators in rhesus monkeys. The efficacy of CEUS in assessing DN in the rhesus monkey was explored. In this study, the TIC was established to obtain the relative quantitative parameters, including AUC, TPH, TTP, PI, and RT. The AUC, which reflects relative blood volume changes in the tissue, showed a linear relationship with tissue blood flow in certain ROIs. Previous research demonstrated that, as the most valuable of all quantitative parameters, the AUC is proportional to the mean blood flow (24). In this study, the AUC was reduced, which suggested that renal blood flow perfusion could have been under low filtration conditions, and blood flow perfusion was clearly decreased. PI, which is proportional to the average blood volume, refers to the most significant signal intensity enhanced by contrast agent in a certain ROI. Since the signal intensity of the contrast agent is significantly correlated with the concentration of microbubbles in a certain ROI, the PI can roughly reflect blood flow, and has a correlation with tissue perfusion. A decrease in the PI value can represent a decline in renal perfusion when renal function is damaged. Combined with pathological results, our data showed that both PI and AUC declined with the deterioration of renal function, which is consistent with the data reported in the literature (25). TTP represents the time from the injection of contrast agent to the maximum signal intensity. This study found that TTP was delayed, which demonstrated that renal perfusion (wash-in) was slowed. The time required for the contrast agent to enter the renal microcapillary bed was extended. Compared with the control group, the extension of TTP appeared as a gentle rise in the lesion group in the TIC. The TPH reflects the microbubbles clearance rate. In this study, the index was shorter in the lesion group than in the control group, suggesting that the microbubbles washed out quickly in the damaged renal tissue. Based on the analysis of these two indicators, the extension of TTP and the shortening of TPH suggested that microvascular perfusion of the renal parenchyma in the lesion group was slower than that in the control group, but clearance was faster.

CEUS can evaluate renal hemodynamic changes noninvasively and repeatedly. Further quantitative evaluation needs experimental verification. There may

be some fundamental limitations to this study. First, the sample size of the experimental animals was small, which may have impacted the results. Second, the perfusion parameters of the CEUS may be influenced by multiple factors, such as the ultrasonic instrument setting, selection of probe, contrast agent concentration and injection speed, as well as the shape, area size, and location of the ROI (26,27). Only experienced reviewers can adequately analyze the perfusion parameters of CEUS. In addition, our study did not grade the degree of renal injury in the lesion group, and the diagnostic efficacy of CEUS at different stages of renal injury in DN warrants further investigation. Although future studies are need to confirmations these results, the preliminary data presented here are encouraging for the use of CEUS as a screening tool in patients with DN.

In conclusion, CEUS may be used to monitor kidney microvascular injury in DN rhesus monkeys. Moreover, CEUS parameters may be used as a supplemental tool for evaluating renal hemodynamic changes in DN.

### Acknowledgments

We thank Xijing Yang and Guangneng Liao from the Animal Experiment Centre of West China Hospital of Sichuan University for their assistance to this work.

*Funding:* This work was supported by the Sichuan Science and Technology Program (No. 2020YFS0211).

### Footnote

*Reporting Checklist:* The authors have completed the ARRIVE reporting checklist. Available at <https://atm.amegroups.com/article/view/10.21037/atm-22-946/rc>

*Data Sharing Statement:* Available at <https://atm.amegroups.com/article/view/10.21037/atm-22-946/dss>

*Conflicts of Interest:* All authors have completed the ICMJE uniform disclosure form (available at <https://atm.amegroups.com/article/view/10.21037/atm-22-946/coif>). WL reports that this work was supported by the Sichuan Science and Technology Program (No. 2020YFS0211). The other authors have no conflicts of interest to declare.

*Ethical Statement:* The authors are accountable for all aspects of the work in ensuring that questions related to the accuracy or integrity of any part of the work are appropriately investigated and resolved. Experiments were

performed under a project license (No. 2018225A) granted by Ethics Committee of West China Hospital of Sichuan University, in compliance with the Guide for the Care and Use of Laboratory Animals, 8th edition.

*Open Access Statement:* This is an Open Access article distributed in accordance with the Creative Commons Attribution-NonCommercial-NoDerivs 4.0 International License (CC BY-NC-ND 4.0), which permits the non-commercial replication and distribution of the article with the strict proviso that no changes or edits are made and the original work is properly cited (including links to both the formal publication through the relevant DOI and the license). See: <https://creativecommons.org/licenses/by-nc-nd/4.0/>.

## References

1. Tziomalos K, Athyros VG. Diabetic Nephropathy: New Risk Factors and Improvements in Diagnosis. *Rev Diabet Stud* 2015;12:110-8.
2. Sagoo MK, Gnudi L. Diabetic nephropathy: an overview. *Methods Mol Biol* 2020;2067:3-7.
3. Ritz E, Zeng XX, Rychlík I. Clinical manifestation and natural history of diabetic nephropathy. *Contrib Nephrol* 2011;170:19-27.
4. Krolewski AS, Warram JH, Christlieb AR, et al. The changing natural history of nephropathy in type I diabetes. *Am J Med* 1985;78:785-94.
5. He M, Wang J, Yin Z, et al. MiR-320a induces diabetic nephropathy via inhibiting MafB. *Aging (Albany NY)* 2019;11:3055-79.
6. Mou X, Zhou DY, Zhou D, et al. A bioinformatics and network pharmacology approach to the mechanisms of action of Shexiao decoction for the treatment of diabetic nephropathy. *Phytomedicine* 2020;69:153192.
7. Yi H, Peng R, Zhang LY, et al. LincRNA-Gm4419 knockdown ameliorates NF- $\kappa$ B/NLRP3 inflammasome-mediated inflammation in diabetic nephropathy. *Cell Death Dis* 2017;8:e2583.
8. Wang YL, Hui YN. The problems that should be noticed in choosing animal models with diabetic retinopathy. *Zhonghua Yan Ke Za Zhi* 2012;48:587-90.
9. Buchanan CE, Mahmoud H, Cox EF, et al. Quantitative assessment of renal structural and functional changes in chronic kidney disease using multi-parametric magnetic resonance imaging. *Nephrol Dial Transplant* 2020;35:955-64.
10. Mahmoud H, Buchanan C, Francis ST, et al. Imaging the kidney using magnetic resonance techniques: structure to function. *Curr Opin Nephrol Hypertens* 2016;25:487-93.
11. Kindgen-Milles D, Slowinski T, Dimski T. New kidney function tests: Renal functional reserve and furosemide stress test. *Med Klin Intensivmed Notfmed* 2020;115:37-42.
12. Ma N, Sun YJ, Ren JH, et al. Characteristics of renal cortical perfusion and its association with renal function among elderly patients with renal artery stenosis. *Zhonghua Xin Xue Guan Bing Za Zhi* 2019;47:628-33.
13. Wang X, Wang S, Pang YP, et al. Contrast-enhanced ultrasound assessment of renal parenchymal perfusion in patients with atherosclerotic renal artery stenosis to predict renal function improvement after revascularization. *Int J Gen Med* 2020;13:1713-21.
14. Wang Y, Li N, Tian X, et al. Evaluation of renal microperfusion in diabetic patients with kidney injury by contrast-enhanced ultrasound. *J Ultrasound Med* 2021;40:1361-8.
15. Wang Y, Zhao P, Li N, et al. A study on correlation between contrast-enhanced ultrasound parameters and pathological features of diabetic nephropathy. *Ultrasound Med Biol* 2022;48:228-36.
16. An X, Liao G, Chen Y, et al. Intervention for early diabetic nephropathy by mesenchymal stem cells in a preclinical nonhuman primate model. *Stem Cell Res Ther* 2019;10:363.
17. He S, Wang C, Du X, et al. MSCs promote the development and improve the function of neonatal porcine islet grafts. *FASEB J* 2018;32:3242-53.
18. Jin X, Zeng L, He S, et al. Comparison of single high-dose streptozotocin with partial pancreatectomy combined with low-dose streptozotocin for diabetes induction in rhesus monkeys. *Exp Biol Med (Maywood)* 2010;235:877-85.
19. Wang D, Liu J, He S, et al. Assessment of early renal damage in diabetic rhesus monkeys. *Endocrine* 2014;47:783-92.
20. Samsu N. Diabetic nephropathy: challenges in pathogenesis, diagnosis, and treatment. *Biomed Res Int* 2021;2021:1497449.
21. Selby NM, Taal MW. An updated overview of diabetic nephropathy: Diagnosis, prognosis, treatment goals and latest guidelines. *Diabetes Obes Metab* 2020;22 Suppl 1:3-15.
22. Stock E, Vanderperren K, Bosmans T, et al. Evaluation of feline renal perfusion with contrast-enhanced ultrasonography and scintigraphy. *PLoS One* 2016;11:e0164488.
23. Lee G, Jeon S, Lee SK, et al. Quantitative evaluation of



- renal parenchymal perfusion using contrast-enhanced ultrasonography in renal ischemia-reperfusion injury in dogs. *J Vet Sci* 2017;18:507-14.
24. Wang L, Mohan C. Contrast-enhanced ultrasound: A promising method for renal microvascular perfusion evaluation. *J Transl Int Med* 2016;4:104-8.
  25. Dong Y, Wang WP, Cao J, et al. Early assessment of chronic kidney dysfunction using contrast-enhanced ultrasound: a pilot study. *Br J Radiol* 2014;87:20140350.
  26. Wilkening W, Lazenby JC, Ermert H. Technique for ultrasound imaging with contrast media using nonlinearity and time variance. *Biomed Tech (Berl)* 1998;43 Suppl:18-9.
  27. Maruyama H, Matsutani S, Saisho H, et al. Grey-scale contrast enhancement in rabbit liver with DMP115 at different acoustic power levels. *Ultrasound Med Biol* 2000;26:1429-38.
- (English Language Editor: J. Teoh)

**Cite this article as:** Wang H, An X, Lu Y, Ling W, Peng Y. Quantitative assessment of renal damage in rhesus monkeys with diabetic nephropathy using contrast-enhanced ultrasound. *Ann Transl Med* 2022;10(6):308. doi: 10.21037/atm-22-946